



FAST Discovery of a Long HI Accretion Stream toward M106

Ming Zhu^{1,2} , Haiyang Yu^{1,2}, Jie Wang¹ , Jin-Long Xu^{1,2}, Wei Du¹ , Lixia Yuan³ , Jing Wang⁴ , Yingjie Jing¹,
Mei Ai^{1,2}, and Peng Jiang^{1,2}

¹ National Astronomical Observatories, Chinese Academy of Sciences, 20A Datun Road, Chaoyang District, Beijing, People's Republic of China; mz@nao.cas.cn, pjiang@nao.cas.cn

² CAS Key Laboratory of FAST, National Astronomical Observatories, Chinese Academy of Sciences, Beijing, People's Republic of China

³ Purple Mountain Observatory and Key Laboratory of Radio Astronomy, Chinese Academy of Sciences, 10 Yuanhua Road, Qixia District, Nanjing 210033, People's Republic of China

⁴ Kavli Institute for Astronomy and Astrophysics, Peking University, Beijing 100871, People's Republic of China

Received 2021 September 29; revised 2021 October 28; accepted 2021 October 29; published 2021 November 22

Abstract

We report the discovery of a possible accretion stream toward a Milky Way–type galaxy M106 based on very deep HI imaging data with the Five-hundred-meter Aperture Spherical radio Telescope (FAST). The accretion stream extends for about 130 kpc in projection length and it is similar to the Magellanic stream in many respects. We provide unambiguous evidence based on the stream morphology, kinematics and local star formation activity to show that the HI gas is being accreted onto the disk of M106. Such a long continuous flow of gas provides a unique opportunity to probe the circumgalactic medium (CGM) and reveals how the gas stream traverses the hot halo and CGM, and eventually reaches the galaxy disk. The source of the stream appears to be from M106's satellite galaxy NGC 4288. We argue that the stream of gas could be due to the tidal interaction with NGC 4288, or with a high speed encounter near this system. Close to the position of UGC 7356 the stream bifurcates into two streams. The second stream may be gas tidally stripped from UGC 7356 or due to an interaction with UGC 7356. Our results show that high-sensitivity HI imaging is crucial in revealing low column density accretion features in nearby galaxies.

Key words: Galaxy accretion – Accretion – Galaxy interactions

Supporting material: animation

1. Introduction

One of the outstanding, unanswered questions in astronomy today is how galaxies accrete enough gas to maintain continuous star formation. It is well known that galaxies assemble their mass in a hierarchical manner by accreting smaller galaxies with their associated stars and dark matter and by merging with other galaxies. While some gas is obtained from satellite galaxies via this hierarchical process, this is only sufficient to fuel continuous star formation in galaxies for a few billion years (Sancisi et al. 2008). Instead, theory predicts that most of the gas is accreted from the intergalactic medium (IGM) in either a hot ($T \sim 10^6$ K) or cold ($T \sim 10^5$ K) phase (Kereš et al. 2005, 2009). Large radio telescopes are capable of detecting the neutral hydrogen in these cold flows via HI emission (Putman 2017 and references therein). However, direct kinematic evidence of gas falling onto a galaxy is relatively rare (Putman 2017).

In order to search for gas accretion in nearby galaxies, we have carried out a HI survey of the local universe with the Five-hundred-meter Aperture Spherical radio Telescope (FAST; Nan et al. 2011). Our survey discovered an archetypical long accretion stream toward M106. This galaxy, also known as NGC4258, is considered to be a Milky Way (MW) analog as it has similar luminosity and Hubble type (Kim et al. 2011). It is in a median-rich environment. M106 is the brightest galaxy in the Canes Venatici (CVn) II cloud, and

it has much more massive satellites than the MW. Spencer et al. (2014) find a total of eight probable low-mass satellites ($-12 < M_v < -17$) within 200 kpc (projected) of M106. The galaxy NGC4144 with $M_B = -18$ is 240 kpc away. Such an environment is similar to that of the M31/M33 system. The MW-type galaxies have only minor interaction with their satellites, and long accretion streams are rarely seen.

In this Letter, we use deep HI imaging with FAST to show that M106 has a long accretion stream extending for about 130 kpc. M106 also has very deep Westerbork Synthesis Radio Telescope (WSRT) imaging from the Hydrogen Accretion in LOcal GALaxieS (HALOGAS) Survey (Heald et al. 2011). Using these two data sets helps to interpret the long HI stream discovered with FAST.

2. Observations and Data Reduction

We have carried out a FAST Extragalactic HI Survey (FEHIS), which is a new survey for HI emission in the northern sky ($61^\circ > \delta > -10^\circ$) over the velocity range -2000 – $20,000$ km s⁻¹, using FAST's focal-plane 19-beam receiver system (Jiang et al. 2019, 2020), which is set in a hexagonal array and works in dual polarization mode, with a frequency range from 1050 MHz to 1450 MHz. For the backend, we choose the Spec(W) spectrometer that has 65,536 channels covering a bandwidth of 500 MHz for each polarization and beam, with a velocity spacing of 1.67 km s⁻¹ and a spectral resolution, after Hanning smoothing, of 4.8 km s⁻¹. The FAST HI survey is carried out with the drift scan mode and the 19-beam receiver was rotated by 23.4° so that the beam tracks are equally spaced in decl. with 1'14" spacing. The FEHIS will eventually cover the entire northern

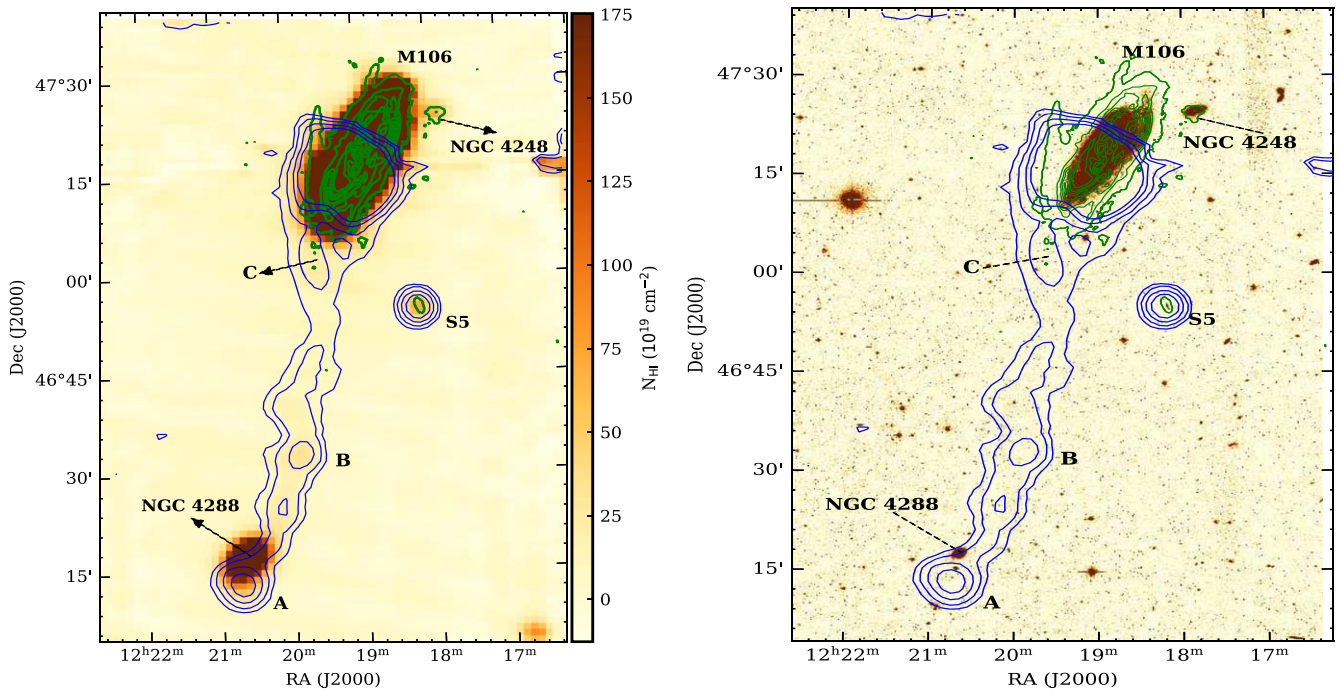


Figure 1. Left: the integrated intensity map of M106 region with the HALOGAS contours overlaid on it. The blue contours are FAST data integrated over $334\text{--}455\text{ km s}^{-1}$ and contour levels are $0.18, 0.36, 0.72,$ and 1.26 Jy km s^{-1} (0.18 Jy km s^{-1} corresponds to $5.2 \times 10^{18}\text{ cm}^{-2}$). Green contours are HALOGAS images (integrated over $200\text{--}750\text{ km s}^{-1}$), contour levels start at 1×10^{19} , and increments by $5.41 \times 10^{20}\text{ cm}^{-2}$. Note the difference in the dynamic range of contours for the galaxy and the stream. The blue contours are selected to highlight the filament, and show only the southern part of the disk. Right: the same contours overlaid on a DECaLS optical image. In both panels, S5 marks the satellite galaxy identified in Kim et al. (2011).

FAST sky at least two times for full sensitivity. The data presented here come from the drift scan observations conducted in 2020 September 25–29 to 2021 July for a total of 12 hr. We have also used the Multibeam on-the-fly (OTF) mode to map the M106 filament regions to confirm the weak detections. The system temperature ranges between $18\text{--}22\text{ K}$ for all beam/polarization channels. The half-power beamwidth (HPBW) was about $2.9'$ at 1.4 GHz for each beam. The pointing accuracy of the telescope was about $10''$ (rms).

Flux calibration was performed by injecting a 10K calibration signal (CAL) every 32 s for a duration of 1 s in order to calibrate the antenna temperature. The data were reduced using the HI FAST data reduction pipeline that was developed by Y. Jing et al. (2021, in preparation) to process the HI data from FAST. Baseline correction was performed using the asymmetrically reweighted penalized least-squares algorithm (Baek et al. 2015), which has been successfully applied to various spectral analyses (Zeng et al. 2021). Once the spectra have been fully calibrated, we apply them to a grid with $1'$ spacing in the image plane, and create the data cube in the standard FITS format. More detailed procedures are described in Xu et al. (2021).

The rms brightness temperature sensitivity is approximately 0.4 mJy beam^{-1} or 6.4 mK per channel, corresponding to a column density sensitivity of $5.6 \times 10^{16}\text{ atoms cm}^{-2}$ in each channel with 4.8 km s^{-1} resolution.

Finally, we check the FAST measured fluxes by comparing with the WSRT fluxes from the blind HI survey of the Canes Venatici region (Kovac et al. 2009), and found good agreement between these two data sets.

3. Results

Figure 1 (left) shows the integrated flux density contours of the HI gas stream detected by FAST overlaid on the integrated intensity (moment-0) map of the M106 region on a grid with $1'$ spacing. The HI filament is integrated over the range $cz = 334\text{--}455\text{ km s}^{-1}$, while the background HI image is integrated over the range of $226\text{--}710\text{ km s}^{-1}$, and shows the galaxy M106 and several of its satellite galaxies. A deep WSRT map from HALOGAS (Heald et al. 2011) is also overlaid on it with green contours, and shows the detailed HI distribution of the galaxy disk with $35''$ resolution. Figure 1 (right) shows the same contours overlaid on a DECaLS optical image (Dey et al. 2019). The FAST contour levels start at $5.2 \times 10^{18}\text{ cm}^{-2}$ (5σ), which is much lower than that of the HALOGAS interferometer map ($1.0 \times 10^{19}\text{ cm}^{-2}$). It reveals a filamentary stream of gas being accreted onto M106. It is remarkable that this HI filament lines up perfectly with the major axis of M106. Such structure does not look like a tidal tail from M106, as most tidal tails from spiral galaxies usually follow the spiral arm direction, such as in the case of NGC262, NGC3356 (Sancisi et al. 2008), M51 (Rots et al. 1990), and the M81 group (Yun et al. 1994). If the gas is stripped away from M106, the gas surface density should decrease with the distance from the disk, which is not the case for M106. Furthermore, tidal interactions between galaxies tend to produce symmetric tails of gas and stars (Toomre & Toomre 1972; Hibbard et al. 2001). In our case the HI filament is not symmetric and no stellar tails are found in the optical image (Figure 1, right). Watkins et al. (2016) have examined the vicinity of M106 to a limiting surface brightness of $m_B = 29.5$ and found no evidence of elongated stellar tidal tails. Thus, the HI filament is most likely an accretion stream toward M106.

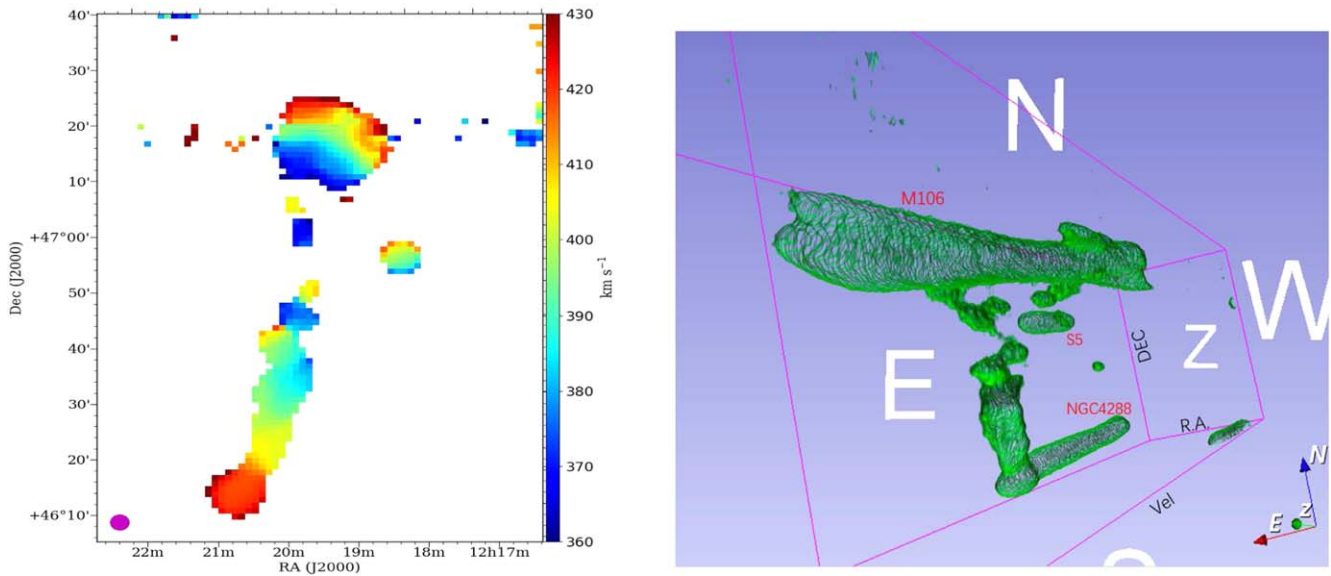


Figure 2. Left: FAST moment-1 map of the M106 H I stream. The pink filled circle indicates a beam size of 3'. Right: a 3D view of the FAST H I data cube for the M106 region. The accretion stream appears as a vertical bar in this image. At the bottom right corner, the arrow E indicates the R.A. direction, N indicates the decl. direction, and Z indicates the velocity direction. An animation of the right panel (lasting for 17 s) showing the full angle view is available. (An animation of this figure is available.)

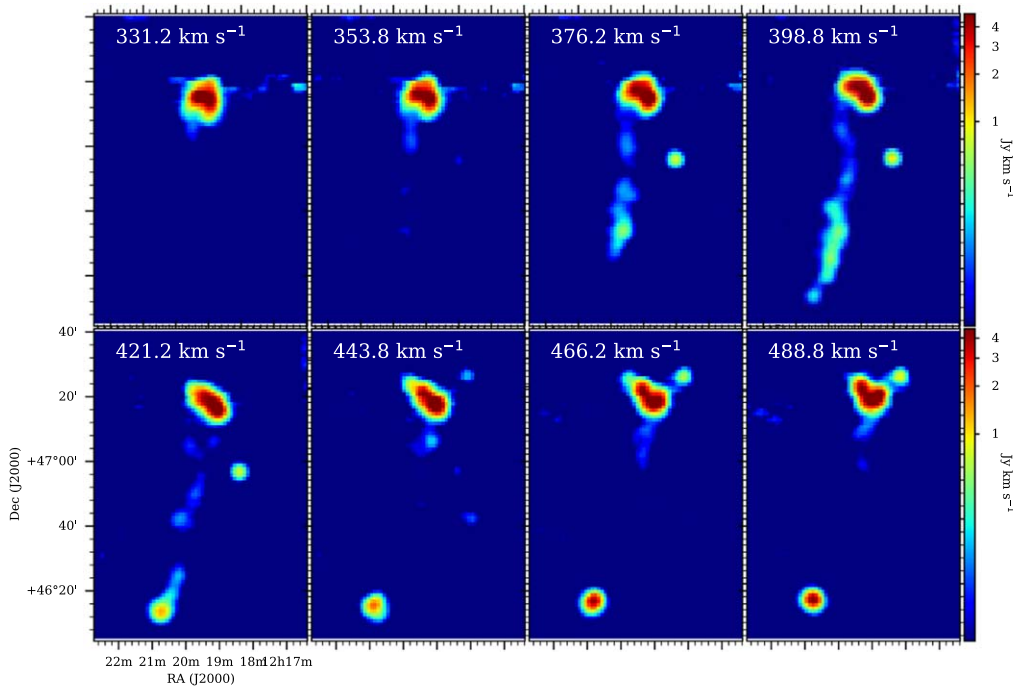


Figure 3. The FAST H I channel map of the M106 region. Each channel is integrated over a velocity range of 22.5 km s^{-1} .

Figure 2 shows the moment-1 map of the stream and a screenshot of a 3D visualization animation of the M106 region. The 3D visualization animation is available online. Figure 3 shows the channel maps of the M106 region. These images show that the H I filament spans a very narrow range ($360\text{--}430 \text{ km s}^{-1}$) in velocity space compared with the galaxy, and it shows a velocity gradient decreasing from the southern to the northern end. The northern end of the H I filament perfectly matches the southern disk of M106 in both space and velocity domain. All these features suggest that a continuous flow of material is being accreted onto M106, probably from its companion galaxies.

At a distance of 7.6 Mpc (Humphreys et al. 2013), the filament is about $60'$ in length, corresponding to a projected length of about 130 kpc. Taylor et al. (2016) list 43 H I features spanning >100 kpc in projected extent. Compared with them, M106 is the most nearby one outside the Local Group. Its proximity provides a good opportunity for detailed studies of the gas accretion process in MW-type galaxies.

Figure 1 shows that the gas stream bifurcates to two substreams when it gets close to the M106 disk. This is most apparent in the bottom left panel of Figure 3 (see also the right panel of Figure 2). In Figure 4 we divide the FAST contours into two parts, the white color part with low velocity ranging

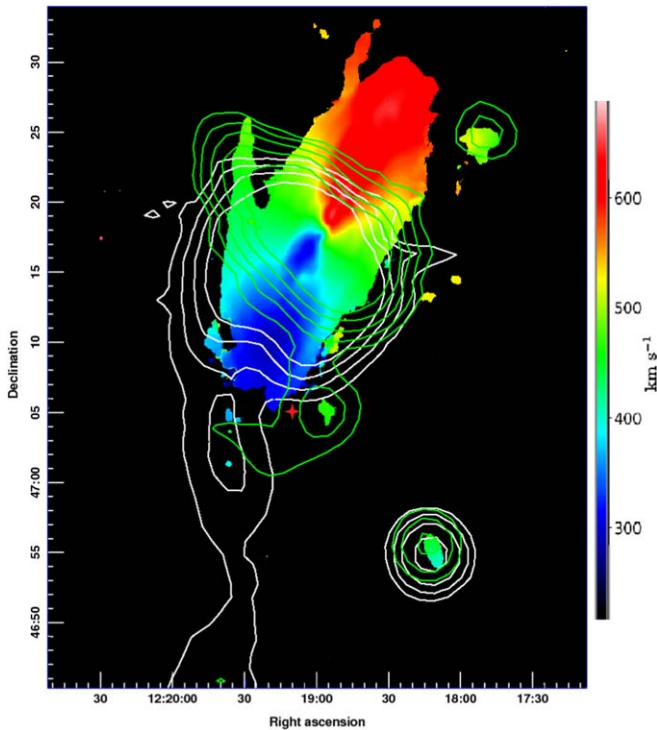


Figure 4. FAST high- and low-velocity contours overlaid on the HALOGAS moment-1 map. The white contours are integrated over $335\text{--}421\text{ km s}^{-1}$; contours levels are 0.2, 0.4, 0.8, and 1.6 Jy km s^{-1} . The green contours are integrated over $421\text{--}465\text{ km s}^{-1}$, and the contour levels are 0.1, 0.2, 0.4, and 0.8 km s^{-1} . The red cross in the high-velocity stream (green contours) marks the position of UGC 7356, a satellite galaxy of M106.

from $334\text{--}421\text{ km s}^{-1}$, and the green color part with a high velocity range of $421\text{--}465\text{ km s}^{-1}$. We can see that in velocity space the accretion stream is actually broken into two streams with different velocities. The background color map of Figure 4 is the moment-1 map of M106 from HALOGAS. From this map we can see that these two streams enter the galaxy envelope from two directions. Furthermore, the HALOGAS map has a high spatial resolution and it reveals several discrete clumps near the southern end of the disk. These clumps are clearly associated with the FAST streams, and different clumps with difference velocities are associated with different substreams, demonstrating good consistency between these two data sets.

We note that the satellite galaxy UGC 7356 is located right in the high-velocity (green contours) stream. This galaxy was classified as an elliptical dwarf galaxy (Bremnes et al. 2000), but in the DECaLS image it appears as a low surface brightness galaxy with a bright core. The optical spectrum from the SDSS survey at the core position yields a velocity of 136 km s^{-1} (Spencer et al. 2014), but this spectrum looks like a stellar spectrum and has been classified as a class STAR spectrum in the SDSS archive, not a class GALAXY spectrum, so the SDSS optical velocity could be questionable. On the other hand, in the channel map at 443.8 km s^{-1} (Figure 3), there is a bright HI concentration near the position of UGC 7356. The center of this HI concentration is offset from the galaxy’s optical center by $1/5$, which is about 3.3 kpc in projection. Thus, it is possible that this HI concentration (with HI mass of $5 \times 10^6 M_{\odot}$) is indeed part of the gas stripped from UGC 7356. It is also possible that part or all of the HI substream with a velocity of $420\text{--}465\text{ km s}^{-1}$ could have originated from this

galaxy. Nevertheless, there is still a possibility that UGC 7356 tidally interacts with M106 and the accretion stream, resulting in the splitting in the stream directions and velocities. Indeed, Watkins et al. (2016) find signs of tidal interaction with UGC 7356 based on deep optical images and they also note that there are extra gas enhancements in the southernmost end of M106 disk outside a $670''$ (24.6 kpc) ring, which could be the result of gas accretion.

Figure 5 shows the HI contours overlaid on the GALEX NUV image. It shows two chains of UV stellar clusters near the anchor point of the accretion stream, indicating induced star formation due to gas accretion. This phenomenon is also noticed by Watkins et al. (2016), and it is the strongest evidence supporting the gas infall scenario instead of tidal tails, as tidal streams should not be correlated with local star formation. The NUV radiation traces star formation of 100 Myr ago; thus, the gas accretion should have lasted for at least 100 Myr. Using Equation (10) and similar parameters from Taylor et al. (2016), we can estimate that the evaporation time is about 1.4 Gyr for HI filaments with a 10 kpc width (assuming an IGM temperature of 10^7 K). Thus, the neutral gas stream can last long enough to be accreted into the galaxy.

We measure a total integrated flux of 483 Jy km s^{-1} , or HI mass of $6.6 \times 10^9 M_{\odot}$ for M106, which is consistent with that from van Albada (1980) and from the HALOGAS measurement ($6.5 \times 10^9 M_{\odot}$ after primary beam attenuation correction; Patterson 2011). The mass of the accretion gas around M106 (clump C area) is $2 \times 10^7 M_{\odot}$. The HI stream has a total HI mass of $1.7 \times 10^8 M_{\odot}$, similar to that of the Magellanic stream. The neutral gas accretion rate is about $0.16 M_{\odot}\text{ yr}^{-1}$ estimated with the formula $dM/dt (M_{\odot}\text{ yr}^{-1}) = Mv/z$, where M is the mass of the accreting material, v is its velocity which is assumed to be 100 km s^{-1} here, and z is the height the material is falling from, which is about 13 kpc from Figure 1(a). If a large portion of the gas is ionized, the total gas accretion rate would be much higher.

4. Discussion

4.1. Possible Origin of the M106 Filament

HI tails with more than 120 kpc have been found in strongly interacting galaxy pairs or in galaxy cluster environments (Appleton et al. 1987; Haynes et al. 2007; Koopmann et al. 2008; Taylor et al. 2016; Leisman et al. 2016; Lee-Waddell et al. 2019; Oosterloo et al. 2018; also in the Rogues Gallery Hibbard et al. 2001), but rarely have been found in MW-type galaxies. M106 is weakly interacting with its satellite galaxies that are more than two orders of magnitude less massive than it (Spencer et al. 2014). Along the direction of the HI stream the most massive galaxy is NGC 4288, which is a Magellanic-type galaxy and is 130 kpc away from M106. It has a stellar mass and dynamical mass similar to that of the Large Magellanic Cloud (LMC), and it appears to connect with the HI stream both in velocity and spatially. Thus, the HI stream between M106 and NGC 4288 could be similar to the Magellanic stream in origin.

Wilcots et al. (1996) have mapped the NGC 4288 area using the Very Large Array (VLA) and found a HI gas cloud outside the NGC 4288 disk, which was dubbed as NGC 4288B, corresponding to clump A in Figure 1(a). They also find a tidally disrupted HI stream extended toward the northeast of NGC 4288. This is confirmed by the Green Bank Telescope

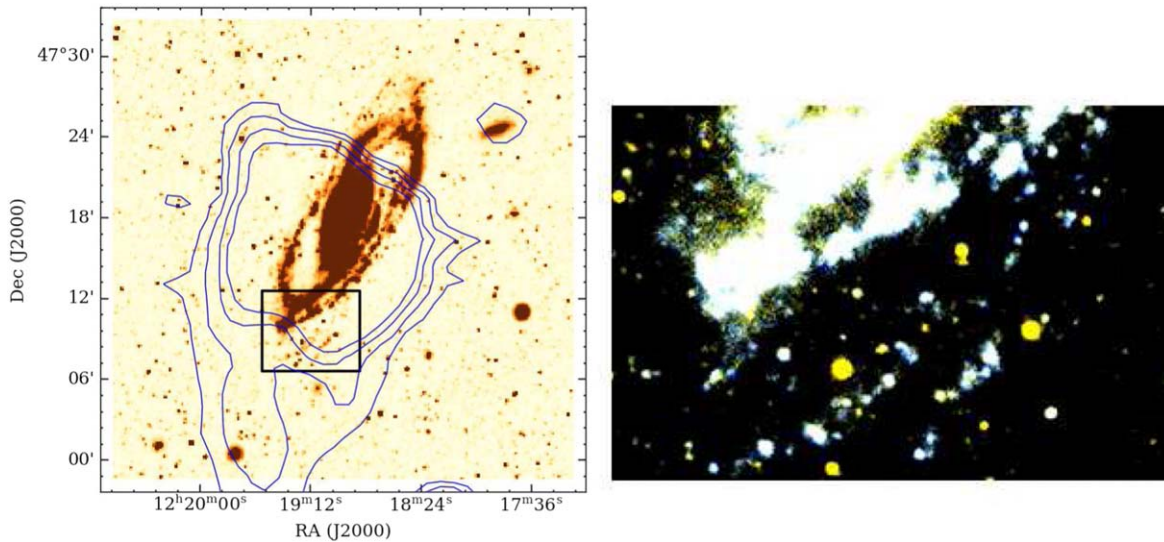


Figure 5. Left: the H I contours overlaid on the GALEX NUV image obtained from the GALEX archive (<http://galex.stsci.edu/GR6/>). The black box indicates the region shown in the right panel. Right: the FUV and NUV false-color image constructed from GALEX data; blue denotes FUV data, while yellow denotes NUV data. This enlarged color map shows two chains of young stellar clusters outside the southern spiral arm directly facing the H I accretion stream, indicating local star formation.

(GBT) (Pingel et al. 2021) as well as by the H I Jodrell All Sky Survey (HIJASS; Wolfinger et al. 2013), which found a H I source without an optical counterpart, namely, HIJASSJ 1219+46, corresponding to clump B in Figure 1(a). Kovac et al. (2009) also map the NGC 4288 region with WSRT. They show (WSRT-CVn-61 in their Figure 5) that the H I cloud NGC 4288B appears to be separated from NGC 4288 in both space and velocity domain. However, all the previous observations were not deep enough to detect the connection between NGC 4288 and M106. The very deep HALOGAS observations also had a limited field of view, so they would miss structures that are more than 0.6° away from the center of M106. Thus, these investigators conclude that the H I clouds NGC 4288B and HIJASSJ 1219+46 are associated with NGC 4288. Our FAST map clearly detects the link between NGC 4288B and the H I filament near M106. Both the morphology and kinematics suggest that this filament is being accreted toward M106.

Kovac et al. (2009) have carried out follow-up optical observations toward the NGC 4288 field down to the surface brightness limit of $26.3 \text{ mag arcsec}^{-2}$ in R and $27.4 \text{ mag arcsec}^{-2}$ in the B band, and no optical counterpart was found for NGC 4288B. Based on these detection limits we can estimate an upper limit of $\sim 10^6 M_\odot$ for the stellar mass component of NGC 4288B (see the Appendix for details). Thus, this object could be a low surface brightness galaxy or a pure H I cloud. In the latter case, it is most likely a tidal debris of NGC 4288, though it has a relatively high H I column density and has the potential to form a tidal dwarf galaxy in the future. As NGC 4288 is located 130 kpc from M106 where the CGM medium density is quite low, ram pressure alone should not be able to strip most of the gas out of its disk. Tidal gravitational force from M106 should have strong effects on it. It is possible that the tidal interaction between galaxies NGC 4288 and NGC 4288B generates a long tidal tail, which is then accreted by M106, just like the Magellanic stream (Putman et al. 1998) toward the MW. Another possibility is similar to the case for the long H I tail of NGC 4254 (Haynes et al. 2007), which is interpreted as a tidal tail driven by a high speed

encounter passing nearby. Such a scenario was successfully reproduced by numerical simulations (Duc et al. 2008).

A major uncertainty of the tidal origin of the M106 filament is that the distance measurement of NGC 4288 is not accurate enough to put it at the same distance as M106. Karachentsev et al. (2013) estimate a distance of 8.05 Mpc, with more than 20% uncertainty. If NGC 4288 is physically far away from M106 and is not interacting with the H I cloud NGC 4288B, the tidal interaction model would need to find an encounter other than NGC 4288. The galaxy UGC 7408 is about $26'$ or 55 kpc away from NGC 4288B in projection. It has a distance of about 7.28 Mpc (Karachentsev et al. 2013), which is virtually at the same distance as M106. Thus, the H I filament could also be a result of the tidal interaction between NGC 4288B, M106, and UGC 7408. Accurate distance measurements of NGC 4288 and more detailed numerical simulations are needed to reveal the origin of the M106 filament.

5. Conclusion

In conclusion, we have obtained the deepest H I image for the vicinity of M106 with FAST and have discovered a long H I gas stream connecting M106 and its possible satellite galaxy NGC 4288. The stream morphology, kinematics, and local star formation activity all point to the possibility of gas infalling toward the disk edge of M106. This H I stream seems to have originated from NGC 4288, which is a 130 kpc away from M106. Our results show that a MW-type galaxy can capture a large amount of gas from its satellites from a long distance. In the case of M106 and NGC 4288, few signs of interaction are found in optical images; high-sensitivity H I imaging is crucial in revealing this type of low column density accretion structure.

We thank the reviewer for constructive comments that led to a significant improvement of the manuscript. M.Z. acknowledges the support of the National Key R&D Program of China No. 2017YFA0402600. D.W. is supported by the NSFC grant Nos. U1931109, 11733006, and the Youth Innovation Promotion Association, CAS. This research made use of data from

WSRT HALOGAS-DR1. The Westerbork Synthesis Radio Telescope is operated by ASTRON (Netherlands Institute for Radio Astronomy) with support from the Netherlands Foundation for Scientific Research NWO. The Five-hundred-meter Aperture Spherical radio Telescope (FAST) is a National Major Scientific Project built by the Chinese Academy of Sciences. Funding for the project has been provided by the National Development and Reform Commission. FAST is operated and managed by the National Astronomical Observatories, Chinese Academy of Sciences.

Appendix

The Upper Limit for the Stellar Mass of NGC 4288B

As mentioned in Section 4.1, the HI cloud NGC 4288B (Clump A in Figure 1, left) has a HI mass of $1.9 \times 10^7 M_\odot$ (assuming a distance of 7.6 Mpc) with no optical counterpart. Based on the optical detection limits, we could estimate an upper limit for the stellar mass of this optically dark galaxy.

First, we estimate the diameter of the HI disk, D_{HI} , defined at a surface density of $1 M_\odot \text{pc}^{-2}$ of the HI disk from the observed HI mass, based on Equation (2) in Wang et al. (2016), which is an empirical scaling relation between the mass and size of the HI disk of the galaxies. As a result, $\log D_{\text{HI}}$ is estimated to be 0.25 ± 0.02 , where D_{HI} is in units of kpc.

Second, we estimate the optical diameter of the dark galaxy, D_{25} , defined at a surface brightness of $25 \text{ mag arcsec}^{-2}$, from D_{HI} .

In the literature, the distribution of D_{HI}/D_{25} has been examined for galaxies. For example, Broeils & Rhee (1997) show the average $D_{\text{HI}}/D_{25} \sim 1.7 \pm 0.5$ for their data. In Wang et al. (2016), it is claimed that about 10% of their galaxies have an HI size larger than 3 times the optical size. So for this optically dark galaxy, we adopt an assumption of $D_{\text{HI}}/D_{25} = 2.0$, and derive an estimate of $D_{25} = 0.89 \text{ kpc}$, corresponding to $R_{25} = 0.44 \text{ kpc}$ ($R_{25} = D_{25}/2$).

Third, assuming that this optically dark galaxy follows an exponentially radial surface brightness distribution (Equation (A)), and the optical effective radius, R_{eff} , is approximately equal to R_{25} , then we can derive the disk scale length, R_s , of the galaxy ($R_{\text{eff}} = 1.68 R_s$). Additionally, this HI-detected galaxy was roughly $1.5 \times 1'$ in the HI map (Kovac et al. 2009), so the major-to-minor axis ratio, q , is roughly assumed to be $1/1.5 = 0.67$.

Now with the estimated parameters of R_s , q , and the already known optical detection limits ($26.3 \text{ mag arcsec}^{-2}$ in R and $27.4 \text{ mag arcsec}^{-2}$ in B), we can derive a rough estimate of the magnitudes in the R and B bands according to

$$\mu_0 = m + 2.5 \log(2\pi R_s^2 q). \quad (\text{A})$$

As a result, we estimate that this optically dark galaxy would not be brighter than 20.38 mag in R and 21.48 mag in B . With a distance of 7.6 Mpc for this galaxy, we further derive that the upper limit of the luminosity is $0.28 \times 10^6 L_\odot$ in the R band and $0.20 \times 10^6 L_\odot$ in the B band.

Since a considerable amount of HI gas might have been stripped from the dark galaxy due to interactions, it is very likely that the HI size, D_{HI} , is underestimated by the relation of Wang et al. (2016). If D_{HI} turns out to be 2–3 times larger than the previous estimate, the luminosities would be $1.12\text{--}2.53 \times 10^6$ and $0.78\text{--}1.77 \times 10^6 L_\odot$ in the R and B bands. The typical stellar mass-to-light ratios (M^*/L) in the

optical R and B bands are statistically around or less than 1 for late-type disks, or dwarf/irregular galaxies (Faber & Gallagher 1979; Portinari et al. 2004), so we estimate that the stellar mass of this dark galaxy would not exceed about $10^6 M_\odot$.

ORCID iDs

Ming Zhu  <https://orcid.org/0000-0001-6083-956X>

Jie Wang  <https://orcid.org/0000-0002-9937-2351>

Wei Du  <https://orcid.org/0000-0003-4546-8216>

Lixia Yuan  <https://orcid.org/0000-0003-0804-9055>

Jing Wang  <https://orcid.org/0000-0002-6593-8820>

References

- Appleton, P. N., Ghigo, F. D., van Gorkom, J. H., Schombert, J. M., & Struck-Marcell, C. 1987, *Natur*, **300**, 140
- Baek, S. J., Park, A., Ahn, Y. J., & Choo, J. 2015, *Ana*, **140**, 250
- Bremnes, T., Binggeli, B., & Prugniel, P. 2000, *A&AS*, **141**, 211
- Broeils, A. H., & Rhee, M. H. 1997, *A&A*, **324**, 877
- Dey, A., et al. 2019, *AJ*, **157**, 168
- Duc, P., Bournaud, F., & Brinks, E. 2008, in Proceedings of the International Astronomical Union, IAU Symposium 244, Dark Galaxies and Lost Baryons, ed. J. I. Davies & M. J. Disney (Cambridge: Cambridge Univ. Press), 216
- Faber, M., & Gallagher, J. S. 1979, *ARA&A*, **17**, 135
- Haynes, M. P., Giovanelli, R., & Kent, B. R. 2007, *ApJ*, **665**, L19
- Heald, G., Jozsa, G., Serra, P., et al. 2011, *A&A*, **526**, 118
- Hibbard, J. E., van Gorkom, J. H., Rupen, M. P., & Schiminovich, D. 2001, in ASP Conf. Ser. 240, Gas and Galaxy Evolution (San Francisco, CA: ASP), 657
- Humphreys, E. M. L., Reid, M. J., Moran, J. M., Greenhill, L. J., & Argon, A. L. 2013, *ApJ*, **775**, 13
- Jiang, P., Tang, N. Y., Hou, L. G., et al. 2020, *RAA*, **20**, 28
- Jiang, P., Yue, Y. L., Gan, H. Q., et al. 2019, *SCPMA*, **62**, 959502
- Karachentsev, I. D., Makarov, D. I., & Kaisina, E. I. 2013, *AJ*, **145**, 101
- Kereš, D., Katz, N., Fardal, M., Davé, R., & Weinberg, D. H. 2009, *MNRAS*, **395**, 160
- Kereš, D., Katz, N., Weinberg, D. H., & Davé, R. 2005, *MNRAS*, **363**, 2
- Kim, E., Kim, M., Hwang, N., et al. 2011, *MNRAS*, **412**, 1881
- Koopmann, R. A., Giovanelli, R., & Haynes, M. P. 2008, *ApJL*, **682**, L85
- Kovac, K., Oosterloo, T. A., & van der Hulst, J. M. 2009, *MNRAS*, **400**, 743
- Lee-Waddell, K., Koribalski, B. S., Westmeier, T., et al. 2019, *MNRAS*, **487**, 5248
- Leisman, L., Haynes, M. P., Giovanelli, R., et al. 2016, *MNRAS*, **463**, 1692
- Nan, R., Li, D., Jin, C., et al. 2011, *IJMPD*, **20**, 989
- Oosterloo, T. A., Zhang, M. L., Lucero, D. M., & Carignan, C. 2018, arXiv:1803.08263
- Patterson, M. 2011, The WSRT HALOGAS Survey: HI Observations of NGC 5055 <https://www.mpa.mpg-garching.mpg.de/gas2011/posters/Patterson.pdf>
- Pingel, N. M., Pisano, D. J., Ruzindana, M., et al. 2021, *AJ*, **161**, 163
- Portinari, L., Sommer-Larsen, J., & Tantaló, R. 2004, *PASA*, **21**, 144
- Putman, M. E. 2017, in Gas Accretion onto Galaxies, Astrophysics and Space Science Library, **430**, ed. A. J. Fox & R. Davé (Berlin: Springer), 1
- Putman, M. E., Gibson, B. K., Staveley-Smith, L., et al. 1998, *Natur*, **394**, 752
- Rots, A. H., Bosma, A., van der Hulst, J. M., Athanassoula, E., & Crane, P. C. 1990, *AJ*, **100**, 387
- Sancisi, R., Fraternali, F., Oosterloo, T., & van der Hulst, T. 2008, *A&ARv*, **15**, 189
- Spencer, M., Loebman, S., & Yoachim, P. 2014, *ApJ*, **788**, 146
- Taylor, R., Davies, J. I., Jachym, P., et al. 2016, *MNRAS*, **461**, 3001
- Toomre, Alar., & Toomre, J. 1972, *ApJ*, **178**, 623
- van Albada, G. D. 1980, *A&A*, **90**, 123
- Wang, J., Koribalski, B., Serra, P., et al. 2016, *MNRAS*, **460**, 2143
- Watkins, A. E., Mihos, J. C., & Harding, P. 2016, *ApJ*, **826**, 59
- Wilcots, E. M., Lehman, C., & Miller, B. 1996, *AJ*, **111**, 1575
- Wolfinger, V. A., Kilborn, V. A., Koribalski, B. S., et al. 2013, *MNRAS*, **428**, 1790
- Xu, J. L., Zhang, C. P., Yu, N. P., et al. 2021, arXiv:2109.06430
- Yun, M. S., Ho, P. T. P., & Lo, K. Y. 1994, *Natur*, **372**, 530
- Zeng, Q. G., Chen, X., Li, X. R., et al. 2021, *MNRAS*, **500**, 2969